Energy-Resolved Field Ion Spectroscopy of Surface Reactions: H2/O2 and H2/H2O on Platinum

B. Sieben, G. Bozdech, N. Ernst

JOURNAL DE PHYSIQUE IV
Colloque C5, supplément au Journal de Physique III, Volume 6, septembre 1996

Energy-Resolved Field Ion Spectroscopy of Surface Reactions: H_2/O_2 and H_2/H_2O on Platinum

B. Sieben, G. Bozdech and N. Ernst

Fritz-Haber-Institut der Max-Planck-Gesellschaft, Faradayweg 4-6, 14195 Berlin, Germany

Abstract. Applications of field ion mass and appearance energy spectroscopy on catalytic surface reactions are reviewed. The investigations have been stimulated by in-situ FIM observations in the group of the late J.H. Block suggesting that single, active sites can be visualized. We have especially examined the energetics and kinetics of H_2-O_2 and H_2-H_2O reactions on [001] oriented Pt-tips. For single surface sites field ion yields have been measured as a function of H_2 partial pressure showing (different) hysteresis behavior for both reaction systems. For H_2/O_2/Pt the results agree qualitatively with features earlier observed at field-free conditions. This finding and the different kinetics of the two reaction systems suggest a less pronounced influence of the applied electric field on the surface catalyzed H_2O formation for H_2/O_2/Pt. At distinct control parameter (pressures, temperature) dynamic phenomena, such as kinetic instabilities and oscillating reaction diffusion fronts, were characterized by probe hole FIM combined with FIMS and FIAPS. For H_2/O_2/Pt comparative measurements have recently revealed a different behavior in FIM and FEM modes possibly caused by the different facets contributing to FI and FE emission currents.

1. INTRODUCTION

Basic research in the area of heterogeneous catalysis has a long-standing tradition in physical chemistry. There are a lot of technological applications, like in the purification of exhaust gases of cars and power plants. Much efforts have been and are still being devoted to the characterization of the molecular processes underlying surface catalyzed reactions, such as the ammonia-synthesis and carbon monoxide oxidation. Recently, pioneering *in-situ* observations on surface catalyzed reactions, using FEM in Leiden in the group of Nieuwenhuys [1] and using FIM in Berlin in the group of Block [2], have opened a novel application of field emission techniques. These efforts aimed at the identification of single reactive sites at catalytic active surfaces and at the characterization of nonlinear surface phenomena, such as kinetic instabilities reported by Voss and Kruse [3] and oscillating chemical waves described by Block et al. [4] in a recent review. These fascinating new observations prompted field ion spectroscopic investigations, especially in the Berlin group which are reviewed in this contribution. For the (oscillating) NO reduction (by H_2) mass spectrometric results will be reported elsewhere [5]. From their FEM and FIM observations Gorodetskii et al. [6-8] concluded that in the case of the H_2 oxidation (by O_2 over Pt) the ion image is largely produced by the product molecules H_2O, leaving the catalyst surface as presumably H_2O^+. Preliminary, low resolution mass analyses reported by Drachsel, Gorodetskii and Block [9] in fact suggested that conclusion. However, the mass resolution did not allow to distinguish mass number 18 (H_2O^+) from mass number 19 (H_3O^+), which - as we know today [10,11] - is an important prerequisite for the field ion spectroscopic characterization of surface reactions producing H_2O, such as the Pt catalyzed H_2-O_2 reaction.

Like other high-resolution imaging methods, such as STM and electron microscopy, the act of imaging in FIM does effect the object under study to a certain extent. The processes which are relevant here concern effects of the high electrostatic field and field gradients on the adsorption-desorption kinetics and field-induced surface reaction pathways. Aiming to contribute to an experimental characterization of these effects, we have employed a variant of a probe hole FIM-FEM combined with field ion mass spectrometry (FIMS) and field ion appearance potential (energy) spectroscopy (FIAPS) on selected surface reaction systems. In this paper we would like to present FIMS and FIAPS results obtained for the oxidation of H_2 and the (field driven) H_2-H_2O reaction over Pt. The data allow to characterize surface reaction field

desorption pathways and the energetics of ion formation processes (Section 3.1). Such data are also valuable for an understanding of the kinetics of surface reactions and of dynamic surface phenomena which we have also examined by time resolved measurements (Section 3.2).

2. EXPERIMENTAL

The experimental method has been described elsewhere [12-14] and will only shortly be sketched. A differentially pumped UHV chamber houses a probe hole FIM which has been combined with a sixty degree, single-focusing magnetic sector field mass spectrometer followed by an electrostatic, five-electrode retarding potential analyzer (Fig. 1).

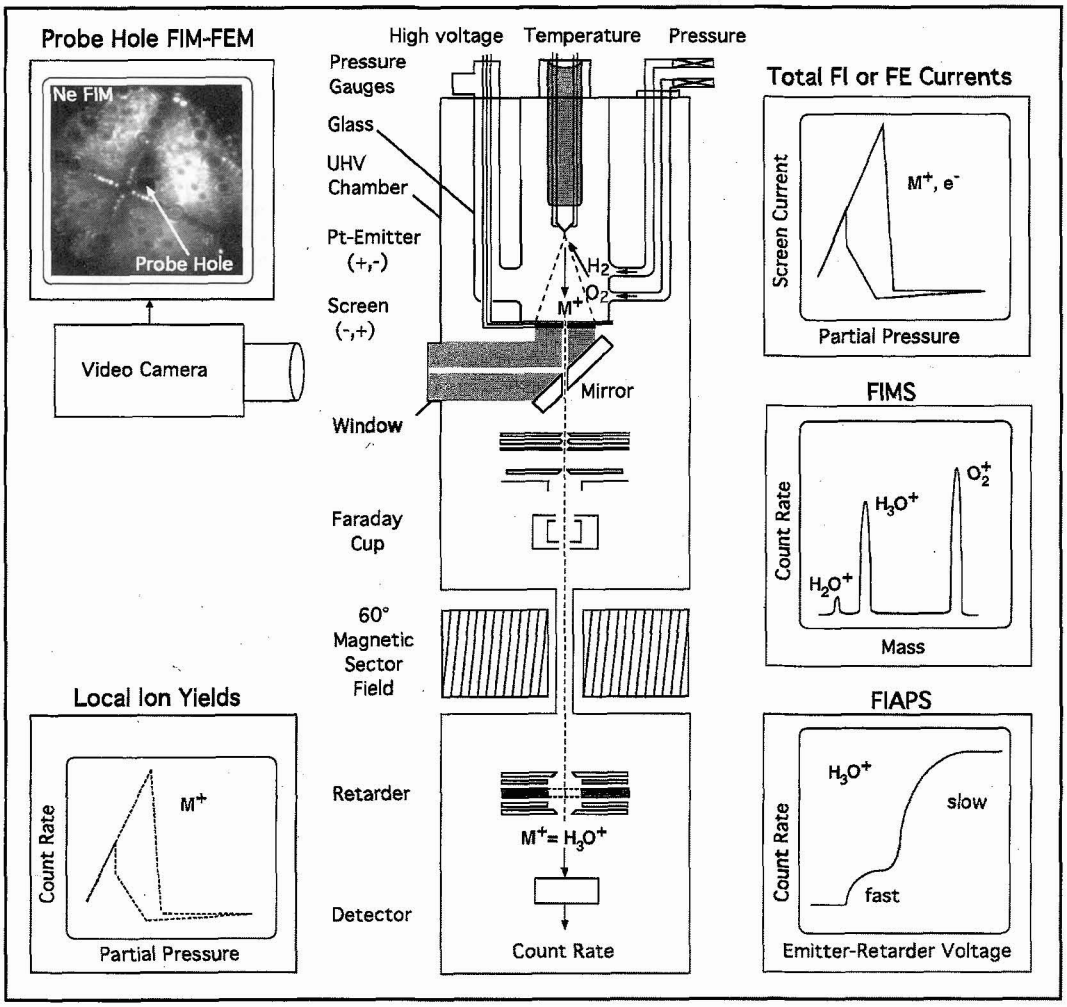

Figure 1: Experimental set-up [12-14]. A glass container houses a probe hole FIM-FEM in a differentially pumped UHV chamber allowing automated measurements of total field ion (FI, upper right panel) and total field electron (FE) currents on the phosphor screen after (channel plate) amplification. For selected surface sites of a field emitter tip such as Pt, *local* ion yields are mass analyzed (right FIMS panel) and energy analyzed (lower right FIAPS panel). Measurements of *total* currents and *local* ion yields (lower left panel) as a function of (H_2 or O_2) partial pressure allow detailed studies of the kinetic behavior of a surface-catalyzed reaction such as $H_2/O_2/Pt$.

The apex of the field emitter (mostly [001] oriented Pt spot-welded on a W wire) acts as a catalyst grain in a flow reactor, e.g. fed with H_2 and O_2. The temperature of the specimens could be controlled between 80 K and 1000 K using a conventional glass coldfinger set-up. To avoid effects of hot filaments pressures of reactive gases were measured with a spinning ball (frictional) manometer. The cleanliness of the gases was controlled in-situ by FIMS which has also been used to characterize the chemical identity of product ion species for single surface sites. Information on the energetics of ion formation was derived from retarding-potential (energy) spectroscopy (FIAPS). Thus, one discriminates between different surface reaction field desorption pathways for a selected ion beam, for example of (slow and fast) H_3O^+ as in the lower right panel of Fig. 1. The dynamics of surface reaction phenomena was imaged by probe hole FIM and FEM. During FIM, ion yields were simultaneously mass and energy analyzed.

During FEM (Fig. 2), electron emission currents (directions of work function changes, $\Delta\Phi$) have also been registered supplementing the kinetic studies, especially for the H_2/O_2/Pt reaction. Using a newly in-

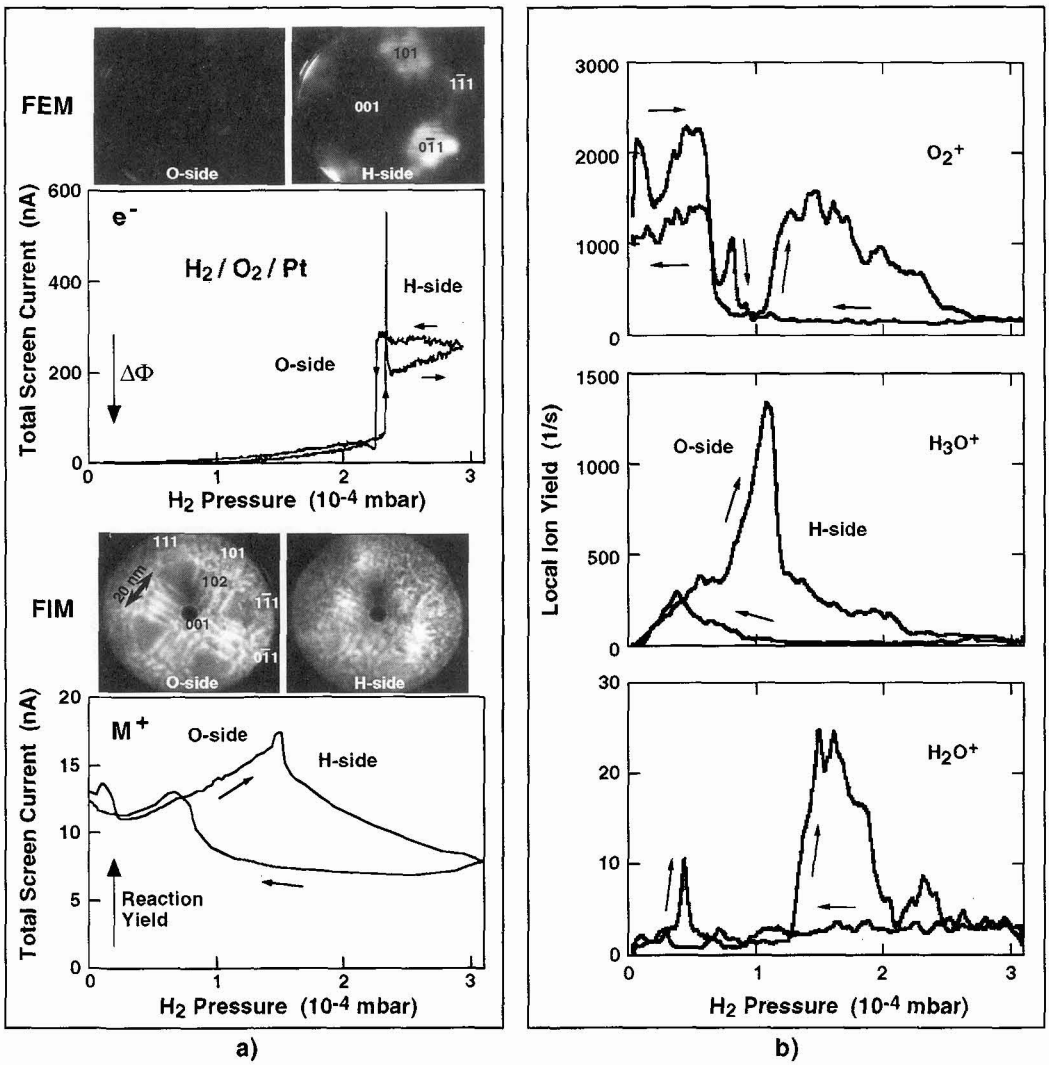

Figure 2: a) Total FE and FI currents and b) local ion yields measured as a function of H_2 partial pressure for H_2/O_2/Pt [14]. In a) the hysteresis behavior differs for FE ($\Delta\Phi$) and FI (reaction yield) measurements. Local ion yields in b) originate from a single site of the striped region in the FIM pattern ($P(O_2) = 5.0 \times 10^{-4}$ mbar, T(Pt) = 360 K, $F(e^-) \approx -0.6$ V/Å, $F(M^+) \approx +1.8$ V/Å, pressure-scan time for each measurement: 2 h 15 min).

stalled computer-assisted data acquisition system, the field ion yields and the field electron emission currents have been measured as a function of automatically varied partial pressures [14]. Fig. 2a) shows H_2 partial pressure dependencies of FEM and FIM video frames and total field electron (e^-, $\Delta\Phi$) and field ion currents (M^+, reaction yields averaged over the tip as a whole) measured on the phosphor screen after amplification by a factor of 10^3. The observed hysteresis behavior differs for FEM and FIM modes which could not be explained by the (differently) field enhanced supply rates for H_2 and O_2 [15]. This difference might have been caused by the different facets contributing to the total FE and total FI currents, respectively. Also, the opening of additional surface reaction field desorption pathways in the FIM mode could have an effect on the kinetics (see Fig. 4b) further below).

Fig. 2b) shows local ion (reaction) yields successively analyzed as a function of H_2 partial pressure. For different species such as O_2^+, H_3O^+ and H_2O^+ there is, albeit different, hysteresis behavior. From such data it was concluded that the maximum of the total FI current (total reaction yield) is dominated by the emission of H_3O^+. Transitions from the O- to the H-side (and vice versa) shift to higher H_2 pressure with increasing temperature for results shown in a) and b).

3. RESULTS AND DISCUSSION

3.1 Energetics and pathways: $H_2/O_2/Pt$

The two field ion pattern in Fig. 3 show a [001]-oriented platinum tip acting as a catalyst grain during the oxidation of hydrogen. The control parameter (T(Pt), $P(H_2)$, $P(O_2)$) have been chosen to achieve a view at the surface at (i) low reactivity (H-side) visualized in the upper video frame and at (ii) high reactivity

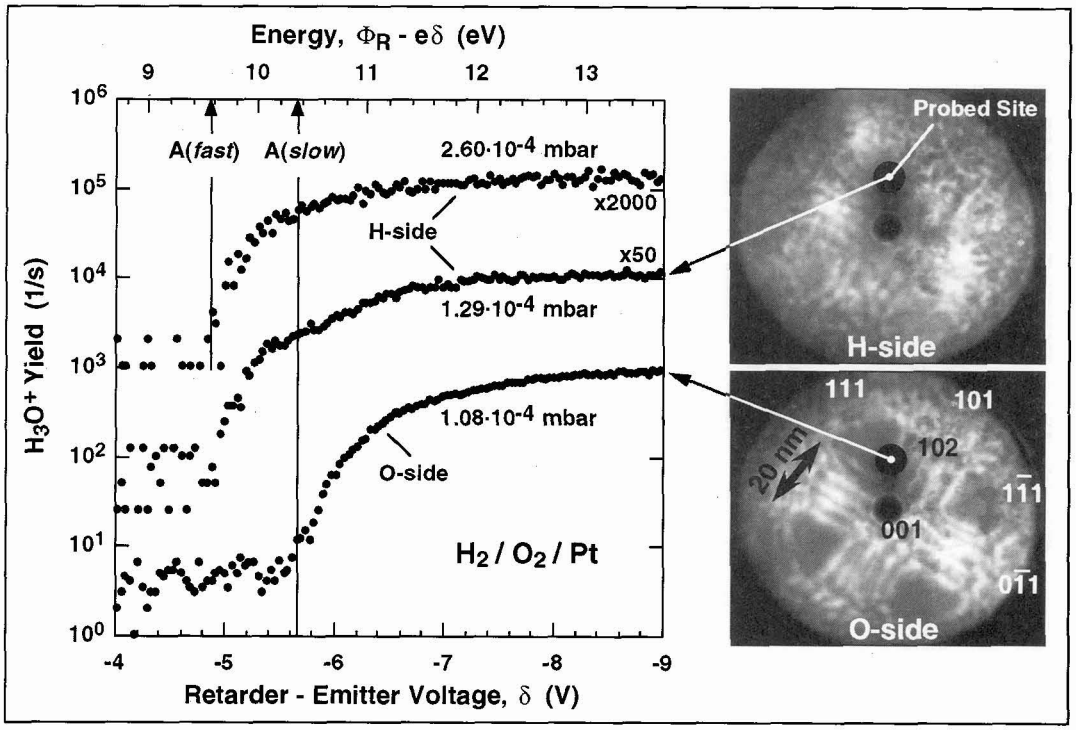

Figure 3: FIAPS (left) and FIM (right) during the H_2 oxidation reaction over Pt [18]. The lower H_3O^+ retardation curve (appearance energy, A(*slow*)) was measured at $P(O_2) = 5.0 \times 10^{-4}$ mbar and at $P(H_2) = 1.08 \times 10^{-4}$ mbar (T(Pt) = 360 K, $F \approx +1.8$ V/Å); the FIM pattern shows a highly reactive surface (O-side) characterized by a cross-like structure. The stepped curve in the middle (A(*fast*) *and* A(*slow*)) was measured at slightly higher H_2 pressure (H-side, FIM: cross-like structure has almost disappeared). The retardation curve on top, measured at highest H_2 pressure reveals no discernible step structure (A(*fast*)). The energy scale was calibrated using an experimentally determined value of the retarder work function, Φ_R.

(O-side) visualized in the lower video frame. At conditions specified for the O-side, H_3O^+ was the most abundant product species in the field ion mass spectrum [10,11]. Using FIMS as shown in Fig. 1, we have detected an O_2^+ signal produced by field ionization of O_2 and field-induced surface reactions of water [16,17]. To contribute to an elucidation of surface reaction field desorption pathways for H_3O^+ formation, FIAPS was employed in detailed studies [11,18]. Fig. 3 shows semi-logarithmic plots of H_3O^+ retardation curves measured at constant O_2 and at three different H_2 pressures. The scale on top has been calibrated using an in-situ measured value for the work function of the retarder electrode for determination of the field ion appearance energy (A) obtained from the onset of a retardation curve [19].

Below a critical H_2 partial pressure we measured A(*slow*) ≈ 10.4 eV (O-side, H_3O^+ retardation curve on the bottom in Fig. 3). A shift to *lower* H_3O^+ appearance energy, i.e. *higher* kinetic energy of approximately 0.8 eV was observed as the H-side was reached, A(*fast*) ≈ 9.6 eV (H_3O^+ retardation curve in the middle). Just above the critical H_2 pressure, a step structure was detected characterizing two peaks in the H_3O^+ energy distribution. As the H_2 pressure was further increased the low kinetic energy peak with A(*slow*) ≈ 10.4 eV disappeared (H_3O^+ retardation curve on top). We note that the phenomena observed by FIM and FIAPS were completely reversible as the H_2 pressure was lowered again, involving hysteresis behavior [18]. The appearance and disappearance of fast H_3O^+ was used to characterize different kinetic regimes as will be discussed later. Thereby, the appearance energy data have provided valuable information on the energetics of surface reaction field desorption pathways [11].

The energy diagram in Fig. 4a) illustrates our current interpretation of the H_3O^+ appearance energy, A(*fast*) ≈ 9.6 eV measured for the H-side of the H_2 oxidation reaction. Detailed mass and energy resolved measurements including isotope exchange experiments have proven a surface reaction field desorption pathway for H_3O^+ formation which involves chemisorbed H from dissociative adsorption of H_2 and field-adsorbed, presumably more strongly bound H_2O. Our data suggest a distinct shift to lower total energy

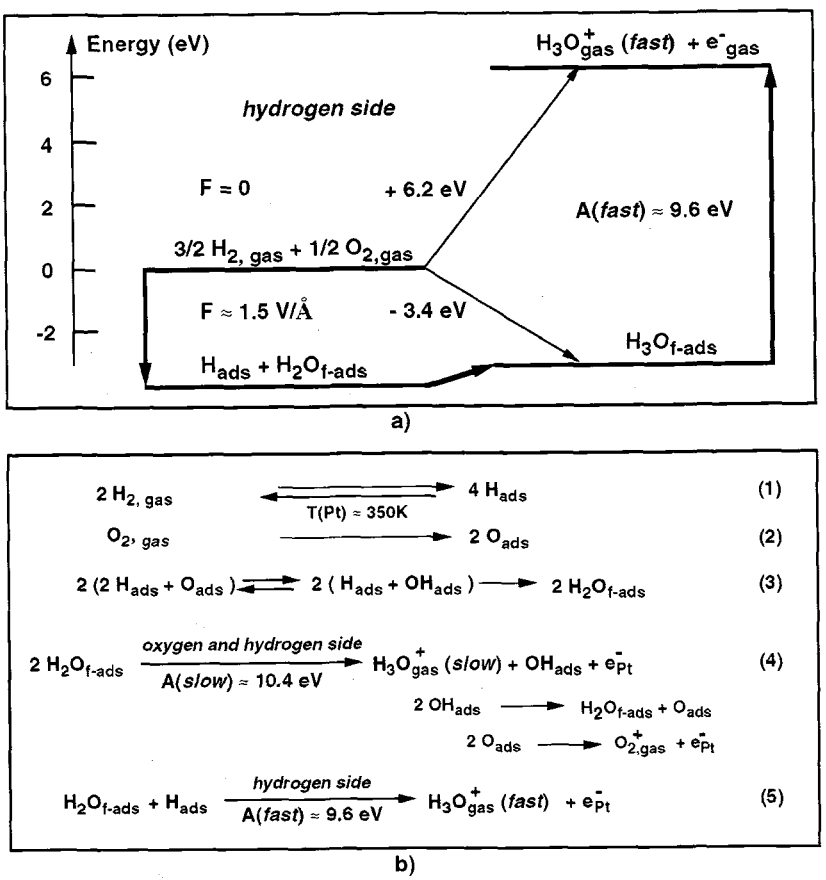

Figure 4: Energetics and reaction pathways for the H_2 oxidation relevant for FIM observations at F ≈ 1.5 V/Å [11,18]. a) On the *hydrogen side* formation of H_3O^+ involves chemisorbed H, field adsorbed H_2O and possibly field adsorbed H_3O as an intermediate. The energy level for H_{ads} + $H_2O_{f\text{-}ads}$ is not accurately known at present. b) Field adsorbed H_2O is formed following LH reaction steps (1)-(3). *Slow* H_3O^+ is the product of a field induced proton transfer between two water molecules (step (4), A(*slow*) ≈ 10.4 eV)). *Fast* H_3O^+ is exclusively detected on the hydrogen side (A(*fast*) ≈ 9.6 eV).

for adsorbed water. This shift includes the long-range polarization and the short-range, field-modified binding energy. Thermal field desorption of H_3O^+ from an intermediate field adsorbed H_3O species appears conceivable. Following the energetic model consideration as in Fig. 4a), the initial state relevant for appearance energy analysis is given by a field adsorbed H_3O at the instant of field desorption over a Schottky hump [11,13]. For the O-side of the kinetic regime slow H_3O^+ species were exclusively measured (A(*slow*) ≈ 10.4 eV) suggesting a reaction pathway proposed earlier by Heinen, Röllgen and Beckey [20]. This pathway mainly involves the field induced proton transfer between two water molecules but additional pathways contributing with smaller rates are still under discussion [17]. On the O-side the H_3O^+ appearance energy is greater, thus the formation of H_3O^+ would be less favored in this kinetic regime. However, the actual yield of H_3O^+, which is in fact at its maximum on the O-side, is governed by kinetic effects which largely depend on the partial surface coverage of adsorbed species like H, O and OH.

To conclude this section, we would like to discuss adsorption, desorption and reaction steps which are in line with the ion spectroscopic results [4]. The first three reaction pathways in Fig. 4b) describe a Langmuir-Hinshelwood (LH) reaction mechanism for the Pt catalyzed H_2O formation from H_2 and O_2. This mechanism has been suggested from experiments on field-free single crystal facets [21]. Reactions (4) to (5) of Fig. 4b) describe (presumably very fast) surface reaction field desorption pathways giving H_3O^+ used to "probe" the formation rate of field adsorbed H_2O [4]. As indicated in the reaction sequence (4) of Fig. 4b) it is conceivable that hot O_{ads} are produced in a disproportionation reaction. These hot O_{ads} are thermally field desorbed as O_2^+, possibly mediated via a field induced molecular precursor state [22]. A new reaction pathway for H_3O^+ formation invoked by Drachsel and Wesseling [17] considers the reaction between adsorbed, intermediate H_2O_2 and OH species. Their H_3O^+-O_2^+ ion coincidence data suggest that such a pathway contributes less than 10% to the total H_3O^+ yield. A clarification of the details involved in the surface reaction field desorption processes (producing *slow* H_3O^+) deserves further experimental and theoretical investigations, if realistic kinetic models are to be developed. In spite of this we have attempted to characterize the kinetic and dynamic behavior for two selected reaction systems discussed in the next section.

3.2 Kinetics and dynamics: H_2/O_2/Pt and H_2/H_2O/Pt

To characterize the kinetics of the H_2/O_2/Pt reaction system we have especially examined the H_2 partial pressure dependence of the H_3O^+ yield for a single surface site [18]. Fig. 5 shows two FIM pattern obtained during local H_3O^+ yield measurements (upper data in the double-logarithmic plot on the right of Fig. 5). This particular result was obtained from a fit through single measurement points taken as a function of H_2 pressure. Starting on the O-side (A(*slow*) ≈ 10.4 eV, pathway (4) of Fig. 4b)), the local, *slow* H_3O^+ yield increased until the H_2/O_2 pressure ratio reached a value of approximately 0.25 where the yield showed a sudden jump to lower values of *slow and fast* H_3O^+ (H-side, A(*fast*) ≈ 9.6 eV, pathway (5) of Fig. 4b)). When the H_2 pressure was further increased we measured even smaller, exclusively fast H_3O^+ yields in a regime where hydrogen "poisoned" the catalytic activity. Lowering the H_2 pressure again, revealed hysteresis behavior; at an H_2/O_2 pressure ratio of 0.20 the reaction system was still on the H-side characterized by the emission of fast H_3O^+. Hysteresis behavior was also observed in the FIM pattern in Fig. 5. Actually, the two images were observed at the same H_2/O_2 pressure ratio (the upper for increasing, the lower for decreasing H_2 partial pressure).

The hysteresis behavior measured for a Pt-tip was compared with results earlier reported for the H_2 oxidation over a macroscopic Pt-foil [18]. Such an experiment was carried out in Moscow by Slin'ko [23] almost 20 years ago and is also shown in Fig. 5. Here, the reaction rate of H_2O formation has been plotted as a function of H_2/O_2 pressure ratio in the same double logarithmic plot as the H_3O^+ results. Although the (field-free) Pt-foil experiment was performed at higher total pressure and temperature, the qualitatively similar features, such as the slope of the reaction yield on the O-side and the occurrence of a hysteresis suggest a relatively small field influence for the field ion emission data. However, there are significant differences, especially in the values of critical pressures and in the hysteresis behavior on the H-side. For selected parameter values, such as partial pressures and temperature, kinetic instabilities involving spatio-temporal fluctuations have been observed. This will be illustrated by an example at the end of this section.

Information on the effect of the applied field strength has also been deduced from a comparison of the H_2 partial pressure dependence of the H_3O^+ reaction yield for the two systems H_2/O_2/Pt and H_2/H_2O/Pt [18]. The latter (field-driven) reaction showed a completely different behavior which was explained by a kinetic model involving the supply of diffusing H from the shank to the apex of the tip [10]. For H_2/H_2O/Pt, we measured a 0-th order dependence of the yield of slow H_3O^+ on H_2 pressure on the "water-side" (until a critical H_2 pressure had been reached). This kinetic regime was dominated by reaction pathway (4) of Fig. 4b); water was directly supplied from gas phase (from an external source) and

produced H_3O^+ during field induced protonation reactions between H_2O molecules at the Pt-tip. The situation differed for the H_2/O_2/Pt system whereby H_2O was formed during LH surface reactions at the apex of the Pt-tip. For the O-side, a reaction order of approximately 1.2 was deduced from H_3O^+-pressure dependencies as in Fig. 5 in good agreement with measured [23] and calculated [21] field free data for H_2O reaction yields. The different kinetic behavior observed for the two reaction systems thus gave a further indication that an external electric field (of approximately 1.5 V/Å) did not influence the kinetics of the H_2/O_2/Pt reaction, at least to a large extent. As a consequence of this reasoning, we used the H_3O^+ yield as a local probe for the characterization of dynamic surface phenomena which could be observed for the two reaction systems at judiciously chosen control parameter.

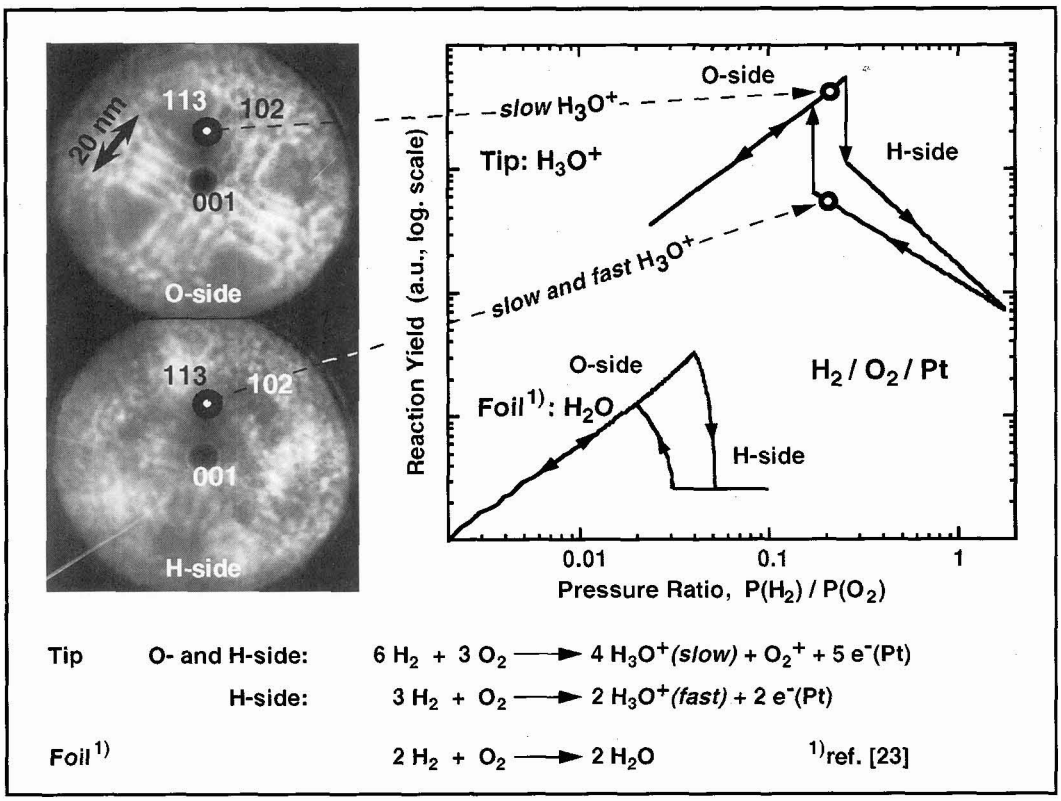

Figure 5: Reaction yields for a Pt-tip: H_3O^+ [18], and a Pt-foil: H_2O [23]. The H_2 partial pressure dependence of the H_3O^+ yield was determined by fitting single data points in a double logarithmic plot. For increasing H_2 pressure a highly reactive state appears at $P(H_2) / P(O_2) \approx 0.2$ (O-side, FIM: bright cross-like structure). Lowering the pressure ratio to ≈ 0.2 establishes hysteresis behavior (H-side, FIM: rather dim, $T(Pt) = 363$ K, $P(O_2) = 5.1 \times 10^{-4}$ mbar, $F \approx 1.5$ V/Å). Earlier results for H_2O formation on a Pt-foil show similar features ($T(Pt) = 408$ K, $P(O_2) \approx 220$ mbar).

It is well known from experimental and theoretical analyses that hysteresis behavior of reaction yields characterizes a nonlinear kinetics for surface-catalyzed reactions far from thermodynamic equilibrium [23-25]. Nonlinear differential equations (including suitable feedback mechanisms) have been employed for describing the functional dependence of surface coverages of reacting species as a function of space and time. Thus, spatio-temporal oscillations and chemical waves have not only been calculated but also imaged with surface analytical tools probing for example work function changes at the micron scale. It was only recently hat FEM [1] and FIM [2-4] studies demonstrated the capability to image such phenomena at higher lateral resolution. We would like to give two examples for these phenomena we have recently analyzed using the energy-resolved ion spectroscopic technique shown in Fig. 1.

At first, we discuss the results of time-resolved probe hole FIM analyses for the H_2/O_2/Pt reaction system (Fig. 6a)). FIM observations of Block, Gorodetskii and Drachsel [7] had already revealed time dependent changes of the brightness in the (001) region of a [001] oriented Pt-tip at selected control parameter. From our kinetic measurements we know that these phenomena can occur on the oxygen side close to the maximum of the H_3O^+ formation rate. Furthermore, appearance energy spectroscopic investigations had shown that at these particular conditions, the slow H_3O^+ were the main reaction product [10-11, 18]. These slow H_3O^+ were most probably formed according to reaction (4) of Fig. 4b), if we neglect other pathways which might have contributed with smaller rates [17]. It was clearly established, that the time dependence of the locally measured slow H_3O^+ yield (right panel of Fig. 6a)) was synchronized with almost periodic brightness changes of the Pt(001) region appearing as a square of approximately 20 nm side length (FIM in Fig. 6a)) [4,18].

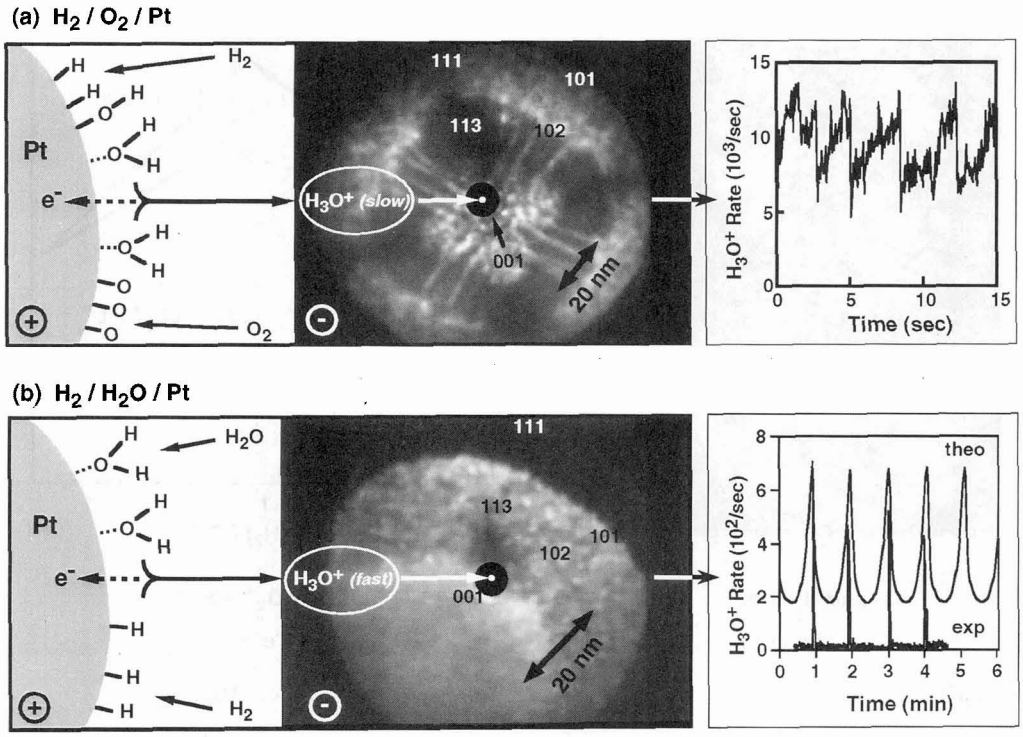

Figure 6: Dynamics (*left*: interpretation, *middle*: probe hole FIM, *right*: local, mass and energy resolved ion yields). a) For H_2/O_2/Pt [18], the brightness of the square shaped emission pattern of the (001) apex-region is time dependent for selected control parameter. The yield of *slow* H_3O^+ shows an almost periodic, sawtooth-like time dependence (T(Pt) = 363 K, $P(H_2) = 1.4 \times 10^{-4}$ mbar, $P(O_2) = 5.1 \times 10^{-4}$ mbar, $F \approx 1.5$ V/Å). b) For H_2/H_2O/Pt [10], reaction-diffusion waves are observed which orignate from regions close to the shank and spread out approximately along [111] zone lines (T(Pt) = 297 K, $P(H_2) = 6.7 \times 10^{-4}$ mbar, $P(H_2O) = 2.6 \times 10^{-6}$ mbar, $F \approx 1.5$ V/Å). Everyother minute a bright front reaches the probe hole, the yield of *fast* H_3O^+ shows outbursts. The measured behavior (exp) has been modeled by a lattice gas approach (theo).

The second example (Fig. 6b)) shows results obtained for the field driven H_2-H_2O reaction system in the oscillating kinetic regime [10]. When a wave front reached the position of the probe hole, the rate of *fast* H_3O^+ *increased* and the rate of *slow* H_3O^+ *decreased*. The fast H_3O^+ were formed in accordance with pathway (5) of Fig. 4b), involving chemisorbed hydrogen and field adsorbed water. The observed spatio-temporal behavior can be viewed as a kind of periodic hydrogen titration reaction which is supported by kinetic lattice gas calculations of Kreuzer and Wang reported in reference [10]. In this model, a flux of atomic hydrogen, mostly from the shank of the tip, reacts with apex-adsorbed O, OH (from reaction

channels such as in the sequence (4) of Fig. 4b)) thus producing field adsorbed H_2O at the apex of the tip. Adsorbed H and H_2O finally yield fast H_3O^+ illustrated in the left panel of Fig. 6b).

Comparisons of the spatio-temporal behavior of the two reaction systems suggested futhermore that the effect of the high electric field on the kinetics of the H_2-O_2 reaction on Pt was relatively moderate. To our knowledge, periodic, spatio-temporal variations of the isothermal water production rate have not been reported on macroscopic Pt single crystals [23]. Gorodetskii et al. [8] concluded that a synergetic effect, produced by the coupling of kinetic properties of adjacent, differently oriented small facets, is a necessary condition for the occurrence of the dynamic phenomena (as in the case of the H_2 oxidation reaction on a Pt-tip). Based on their FIM work on the NO/H_2/Pt system Voss and Kruse [3] pointed out that reaction-induced morphological changes are a further necessary prerequisite for the occurrence of self-sustained kinetic oscillations. Their observations and conclusions are in line with the appearance of a striped FIM pattern such as in Fig. 6a) revealing reaction induced (reversible) surface-structural changes for the H_2/O_2/Pt system. To this end, our combined FIM and ion spectroscopic results support the view of Block, Gorodetskii and Drachsel [7] that such a FIM pattern provides an in-situ image of catalytic active sites at the surface.

Conclusions

For the H_2/O_2/Pt and the (field driven) H_2/H_2O/Pt reaction systems the local yields of product ions, such as H_3O^+ showed markedly different H_2 partial pressure dependencies. These differences and comparisons with earlier experimental and theoretical results suggested that the influence of the applied field ($\approx$ 1.5 V/Å) on the kinetics of the H_2/O_2/Pt reaction was less pronounced. Most recently H_2 pressure dependencies (as presented in section 2) have been measured for H_2/O_2/Pt revealing *different* hysteresis behavior using FEM and FIM. This could have been caused by the different facets actually contributing to the measured FE and FI currents, respectively. Other effects of the applied field might also be important, such as the opening of additional surface reaction field desorption pathways during FIM and a field induced strengthening of the H_2O-Pt interaction. Further FIM and (probe hole) FEM analyses are certainly desirable. Such experimental efforts accompanied by kinetic calculations for H_2/O_2/Pt, along the lines already performed for H_2/H_2O/Pt, could give further insights inasmuch the electrostatic field and field gradients effect FIM observations. At the end we conclude that the field ion microscope can be used for the *in-situ* imaging of single catalytic active sites; but the effects of the field have to be quantified for every system under study.

Acknowledgment

We would like to thank Dr. K. Doblhofer and Professor F. W. Röllgen for helpful discussions.

References

[1] M.F.H. van Tol, A. Gielbert and B.E. Nieuwenhuys, *Catal. Lett.* **16** (1992) 297.
[2] V. Gorodetskii, W. Drachsel and J.H. Block, *Catal. Lett.* **19** (1993) 223.
[3] C. Voss and N. Kruse, *Appl. Surf. Sci.* **87/88** (1994) 127.
[4] J.H. Block, W. Drachsel, N. Ernst, B. Sieben and V. Gorodetskii, *Ber. Bunsenges. Phys. Chem.* **99** (1995) 1363 and references therein.
[5] C. Voss, N. Kruse, G. Abend and J.H. Block, to be published; cited as Ref. [6] by C. Voss and N. Kruse, *Appl. Surf. Sci.* **94/95** (1996) 186.
[6] V. Gorodetskii, J.H. Block and W. Drachsel, *Appl. Surf. Sci.* **76/77** (1994) 129.
[7] J.H. Block, V. Gorodetskii and W. Drachsel, *Recl. Trav. Chim. Pays-Bas* **113** (1994) 444.
[8] V. Gorodetskii, J. Lauterbach, H.-H. Rotermund, J.H. Block and G. Ertl, *Nature* **370** (1994) 276.
[9] W. Drachsel, V. Gorodetskii and J.H. Block, *Appl. Surf. Sci.* **76/77** (1994) 70.
[10] N. Ernst, G. Bozdech, V. Gorodetskii, H.-J. Kreuzer, R.L.C. Wang and J.H. Block, *Surf. Sci.* **318** (1994) L1211.
[11] N. Ernst, G. Bozdech,V. Gorodetskii and J.H. Block, *Int. J. Mass Spectrom. Ion Processes* **152** (1996) 185.
[12] N. Ernst, G. Bozdech and A.J. Melmed, *J. de Physique* C6 **49** (1988) 453.
[13] N. Ernst, *Appl. Surf. Sci.* **67** (1993) 82.

[14] G. Bozdech, B. Sieben and N. Ernst, 43rd International Field Emission Symposium, Moscow, July 14-19 (1996) Program and Abstracts, P-65.
[15] K.D. Rendulic and M. Leisch, *Surf. Sci.* **95** (1980) L271.
[16] W.A. Schmidt, *Z. Naturforsch.* **19a** (1964) 318.
[17] W. Drachsel and C. Wesseling, private communications (1996) and this volume.
[18] B. Sieben, G. Bozdech, N. Ernst and J.H. Block, *Surf. Sci.* **352** (1996) 167.
[19] N. Ernst, W.A. Schmidt, M. Naschitzki and J. Unger, 38th International Field Emission Symposium, Vienna, August 5-9 (1991) Program and Abstracts, 6-2; W.A. Schmidt, N. Ernst and Yu. Suchorski, *Appl. Surf. Sci.* **67** (1993) 101.
[20] H.J. Heinen, F.W. Röllgen and H.D. Beckey, *Z. Naturforsch.* **29a** (1974) 773.
[21] V.P. Zhdanov and B. Kasemo, *Surf. Sci. Rep.* **20** (1994) 111.
[22] B. Sieben, Yu. Suchorski, G. Bozdech and N. Ernst, Z. Physik. Chem. accepted.
[23] M.M. Slin'ko, Ph.D. Thesis, Institute of Petrochemical Synthesis, USSR Academy of Sciences, Moscow 1977 (in Russian), cited as ref.[17] by M.M. Slin'ko and N.I. Jaeger in "Oscillating Heterogeneous Catalytic Systems" in: Studies in Surface Science and Catalysis 86, Advisory Editors B. Delmon and J.T. Yates (Elsevier, Amsterdam 1994), p. 131.
[24] G. Ertl, *Science* **254** (1991) 1750.
[25] R. Imbihl, *Progr. Surf. Sci.* **44** (1993) 185.